Am J Physiol Renal Physiol 293: F1865–F1876, 2007.
First published October 3, 2007; doi:10.1152/ajprenal.00347.2007.

Functional effects of nonsynonymous polymorphisms in the human *TRPV1* gene

Hongshi Xu,[1,2] Wei Tian,[1,2] Yi Fu,[1,2] Terry T. Oyama,[1,2] Sharon Anderson,[1,2] and David M. Cohen[1,2]

[1]*Division of Nephrology and Hypertension, Oregon Health and Science University, and* [2]*Portland Veterans Affairs Medical Center, Portland, Oregon*

Submitted 25 July 2007; accepted in final form 2 October 2007

Xu H, Tian W, Fu Y, Oyama TT, Anderson S, Cohen DM. Functional effects of nonsynonymous polymorphisms in the human *TRPV1* gene. *Am J Physiol Renal Physiol* 293: F1865–F1876, 2007. First published October 3, 2007; doi:10.1152/ajprenal.00347.2007.—The prototypical member of the vanilloid-responsive-like subfamily of transient receptor potential (TRP) channels is TRPV1. TRPV1 mediates aspects of nociception and neurogenic inflammation; however, new roles are emerging in sensation of both luminal stretch and systemic tonicity. Although at least six nonsynonymous polymorphisms in the human *TRPV1* gene have been identified, there has been no systematic investigation into their functional consequences. When heterologously expressed in HEK293 cells, all variants exhibited equivalent EC_{50} for the classic agonist capsaicin. This agonist elicited a greater maximal response in $TRPV1^{I315M}$ and $TRPV1^{P91S}$ variants (relative to $TRPV1^{WT}$), as did a second agonist, anandamide. Expression of these two variants in whole-cell lysates and at the cell surface was markedly greater than that of wild-type TRPV1, whereas expression at the mRNA level was either unchanged ($TRPV1^{P91S}$) or only very modestly increased ($TRPV1^{I315M}$). Incorporation of multiple nonsynonymous SNPs, informed by the population-specific haplotype block structure of the *TRPV1* gene, did not lead to variant channels with unique features vis-à-vis capsaicin responsiveness. Recently, polymorphisms/mutations were identified in two highly conserved TRPV1 residues in the nonobese diabetic (NOD) murine model. Incorporation of these changes into human TRPV1 gave rise to a channel with a normal EC_{50} for capsaicin, but with a markedly elevated Hill slope such that the variant channel was hyporesponsive to capsaicin at low doses (<10 nM) and hyperresponsive at high doses (>10 nM). In aggregate, these data underscore expression-level and functional differences among naturally occurring TRPV1 variants; the implications with respect to human physiology are considered.

capsaicin; single-nucleotide polymorphism; diabetes

THE TRANSIENT RECEPTOR POTENTIAL (TRP) family of channels transmit a broad range of environmental information to the cell interior, generally via calcium entry. Specific TRP channels respond to high and low temperatures, anisotonicity, and an array of tastants, as well as numerous other stimuli (reviewed in Ref. 45). TRP channels are divided into six broad families based on sequence homology (49); the TRPV family is named for its founding member, the vanilloid receptor, or TRPV1.

TRPV1 is a nonselective cation channel (7, 37, 51) that was initially cloned and molecularly characterized as the capsaicin (i.e., "hot pepper") or vanilloid receptor (14). TRPV1 mediates the ion fluxes accompanying exposure of neurons and mucosae to a variety of noxious stimuli. In vitro, TRPV1 is activated by voltage, vanilloid compounds, heat, protons, and a variety of lipid agonists including endogenous cannabinoids (89) and eicosanoids (27). TRPV1 is also activated by zingerone and piperone, compounds lending distinctive pungency to ginger and black pepper, respectively (36, 42). TRPV1 is predicted to have six transmembrane segments (14) and to assemble into a tetrameric structure (33). TRPV1, like other TRPV family members, participates in heteromerization (70).

Capsaicin, as mentioned above, is the prototypical activator of TRPV1; the compound is used therapeutically in desensitization of nociceptive pathways (78). Capsaicin likely traverses the plasma membrane to interact with intracellular site(s) on the channel (30). Initial data suggested involvement of intracellular residues R114 and E761 (31); data derived in part from domain-swapping experiments with the capsaicin-insensitive avian and lapine TRPV1 have implicated the second through fourth membrane-spanning helices and an intervening intracellular loop (21, 29). Interpretation is complicated by evidence for uncoupling of capsaicin binding and actual channel activation, consistent with an allosteric gating mechanism (33). Deletion of a 60-residue cassette from the NH_2 terminus in a naturally occurring human TRPV1 splice variant renders the channel insensitive to capsaicin; the response to noxious heat, however, may be preserved (38, 83). Binding assays and single-channel electrophysiological studies suggest that interaction with at least two capsaicin molecules is required for full channel activation (reviewed in Ref. 61).

Consistent with its role in nociception, TRPV1 is primarily expressed in the dorsal root ganglia and peripheral sensory nerve endings and, to a much lesser extent, in the central nervous system (14, 43, 63). Increasingly, however, TRPV1 has been identified in both healthy and diseased epithelia. TRPV1 is expressed in urethra and bladder (1, 9, 53, 79), including the epithelial cells lining the bladder (9). Mice lacking *TRPV1* ($TRPV1^{-/-}$ mice) exhibited impaired sensation of bladder filling and abnormal reflex voiding (10). TRPV1 is also expressed in nasal and airway mucosa (2, 60, 77, 79, 80) and the gastrointestinal tract (5, 22), where its dysregulation has been implicated in a number of disease states (11, 12, 28, 40, 85). TRPV1 is highly expressed in the kidney (14, 16, 62, 83), along with potentially unique splice variants (14, 16, 62, 81). Although its function remains obscure in this tissue, a pathological role in the uptake of the nephrotoxic antibiotic gentamicin has been suggested (48). TRPV1 also innervates the renal pelvis and mediates the renorenal reflex, wherein

Address for reprint requests and other correspondence: D. M. Cohen, Mailcode PP262, Oregon Health and Science University, 3314 S.W. US Veterans Hospital Rd., Portland, OR 97201 (e-mail: cohend@ohsu.edu).

The costs of publication of this article were defrayed in part by the payment of page charges. The article must therefore be hereby marked "*advertisement*" in accordance with 18 U.S.C. Section 1734 solely to indicate this fact.

elevated intrapelvic pressure (as might accompany unilateral ureteral obstruction) promotes natriuresis via the contralateral kidney (88).

TRPV1, like the closely related TRPV4 (34, 35, 76), is suspected of playing a pivotal role in systemic osmoregulation (67). Hypertonicity activates a cation current in the osmotically sensitive ADH neurons of the supraoptic nucleus; however, corresponding neurons from *TRPV1*$^{-/-}$ mice were unresponsive to this physiological stimulus. In further experiments, a channel exhibiting electrophysiological properties consistent with TRPV1 was identified in these cells. Interestingly, only a portion of TRPV1 mRNA could be PCR amplified from RNA prepared from this tissue (67), and no osmotically responsive variant of TRPV1 has been described to date.

We hypothesized that nonsynonymous polymorphisms of human TRPV1 may confer novel channel properties. We compared known nonsynonymous single-nucleotide polymorphisms (SNPs) to wild-type TRPV1 in vitro through a variety of approaches. Although EC_{50} for capsaicin was similar among the variants, at least two, TRPV1^{P91S} and TRPV1^{I315M}, exhibited increased expression at the protein level. Gene expression level, in contrast to aberrant function, is increasingly recognized as a major manifestation of human genetic variation. In addition, a potentially diabetogenic mutant of human TRPV1 modeled after a diabetogenic murine variant was shown to exhibit a unique capsaicin dose-response relationship.

METHODS

Nonsynonymous polymorphisms in the human TRPV1 gene. We screened SNPs in the *TRPV1* gene appearing in the database at the NCBI website (http://www.ncbi.nlm.nih.gov/projects/SNP/). We chose to focus on six nonsynonymous SNPs in the human *TRPV1* coding region (Fig. 1*A*). Two SNPs in exon 1 were located in the NH_2 terminus of the protein: TRPV1^{K2N} (SNP ID rs9894618) and TRPV1^{P91S}(rs222749). TRPV1^{I315M} (rs222747) affected exon 5 and localized to the region of the ankyrin repeat domains, which are postulated to mediate protein-protein interactions. TRPV1^{T469I} (rs224534), TRPV1^{T505A}(rs17633288), and TRPV1^{I585V} (rs8065080), encoded by exons 8, 9, and 11, respectively, affect the transmembrane domain of the channel. TRPV1^{T469I} is predicted to reside on an extracellular loop between membrane-spanning helices one and two, whereas TRPV1^{T505A} affects an intracellular loop between membrane-spanning helices two and three. The TRPV1^{T505A} site is adjacent to Ser-502, which undergoes regulatory phosphorylation by protein kinase C, protein kinase A, and calmodulin-dependent protein kinase II (reviewed in Ref. 82). A seventh nonsynonymous SNP, rs224496, resulted in a conservative substitution (TRPV1^{D421E}) and exhibited extremely low minor allele frequency (= 0.00 in HapMap; http://www.hapmap.org/); functional studies with this SNP were not pursued. None of these SNPs map to the 60-residue NH_2-terminal cassette absent from the human TRPV1b splice variant, and none (with the possible exception of TRPV1^{T505A}) directly impact regions of the channel implicated in capsaicin binding or response (21, 29–31, 38, 83).

Nonsynonymous TRPV1 SNPs associated with diabetes development in the murine nonobese diabetic (NOD) model (58) were generated on the background of the human TRPV1 cDNA. The two residues affected in the NOD mouse *TRPV1* gene are conserved between mouse and human; we designated the human equivalent hTRPV1$^{P322A/D734E}$. Neither mutant residue affects the transmembrane/ion channel motif in TRPV1. For haplotype analysis, genotyping data reflecting 100 kb, 500 kb, and 1 Mb of chromosome 17 centered on the human *TRPV1* gene were downloaded from the International HapMap Project (http://www.hapmap.org/) and analyzed within Haploview (http://www.broad.mit.edu/mpg/haploview/) (6). For the CEU population, data were converted to the *D′* parameter for linkage disequilibrium for clarity in a grayscale depiction (i.e., see Fig. 8).

Cell culture and transient transfection. HEK293 cells were maintained in DMEM/F12 medium (JRH) supplemented with 10% fetal bovine serum (JRH). All reagents were obtained from Sigma (St. Louis, MO) unless otherwise specified. Agonists and inhibitors were applied as follows: 1–1,000 nM capsaicin, 100 nM epidermal growth factor; 10 nM forskolin, 100 nM phorbol 12-myristate 13-acetate, and 100 nM anandamide. Pretreatment with these agents, where indicated, was applied ~10 min before capsaicin treatment and remained present for the duration of treatment. Cells were transiently transfected with Lipofectamine PLUS (Life Technologies) in accordance with the manufacturer's directions using 15 μl of PLUS reagent, 30 μl of Lipofectamine, and 6 μg of plasmid DNA reagent/100-mm dish of cells. All transfections were performed in parallel into HEK drawn from the same pool of trypsinized cells.

Determination of intracellular calcium. For intracellular calcium assays, cells were passaged on the second day after transfection at 1:1 into poly-D-lysine-coated black-wall, flat-bottom 96-well plates (BioCoat; Becton-Dickinson Labware) at 3–5 × 10^4 cells/well. The following day, cells were loaded with fura 2 [fura 2-AM, 2 μM, plus 0.01% Pluronic-127 in 130 mM NaCl, 4.7 mM KCl, 1.26 mM $CaCl_2$, 1.18 mM $MgSO_4$, 5.6 mM glucose, 20 mM HEPES (pH 7.5); HBSS] for 20 min at 37°C. Cells were washed twice with HBSS and placed in 100 μl/well of HBSS before the assay. Compounds were added in 100-μl volume after baseline readings were established using a FlexStation II (Molecular Devices). Data were collected using an emission wavelength of 510 nm and alternating excitation at 340 and 380 nm at 3.9-s intervals for a total of 2 min. Twelve replicates were performed for each capsaicin dose (1 "row" on a 96-well plate), and eight doses were tested simultaneously (0, 1, 3, 10, 30, 100, 300, and 1,000 nM); this was considered a single experiment for a single TRPV1 variant. A total of five to eight experiments were performed for each variant. Raw data were exported and reduced in Excel (Microsoft) and graphed using Prism software (GraphPad Software). For each concentration of capsaicin, the response (Δfura 2 ratio) was calculated as ($r_{max} - r_{initial}$), where $r_{initial}$ represents the mean of the first two data points, and r_{max} is the maximal fura 2 ratio achieved after treatment. The initial downward deflection in the fura 2 ratio (e.g., in Fig. 1*B*) is an artifact of the agonist injection. A logarithmic dose-response relationship was plotted for each experiment with each TRPV1 variant, and a sigmoidal four-parameter (*top*, *bottom*, EC_{50}, and Hill slope) Hill equation dose-response curve was fit using the nonlinear regression feature of Prism (GraphPad Software). Curves were fit with both a fixed Hill slope of 1 and with a variable Hill slope, and EC_{50} for capsaicin was reported (47).

Cell-surface biotinylation and immunoblotting. Cell-surface biotinylation was performed 48 h after transient transfection. HEK293 monolayers were washed three times with ice-cold PBS, incubated with 0.5 mg/ml Sulfo-NHS-LC-Biotin (Pierce Biotechnology, Rockford, IL) for 30 min at 4°C, quenched by incubation with 100 mM glycine in ice-cold PBS for 30 min at 4°C, and then washed three times with ice-cold PBS. Monolayers were lysed in lysis buffer [125 mM NaCl, 50 mM Tris (pH 7.5), 0.1% SDS, 0.5% sodium deoxycholate, 1% Nonidet P-40, 1 mM sodium orthovanadate, 1 mM 4-(2-aminoethyl)benzenesulfonyl fluoride, 1 μg/ml leupeptin, 1 μg/ml aprotinin, 1 μg/ml pepstatin A, 25 mM β-glycerophosphate, 2 mM sodium pyrophosphate] for 30 min at 4°C. The protein concentrations were determined by the Bradford method (Bio-Rad). Twenty micrograms of whole-cell lysate was set aside for blotting in parallel. To the remaining lysates, ImmunoPure Streptavidin Beads (40 μl; Pierce Biotechnology) were added to ~3 mg of biotinylated protein and the mixture was incubated at 4°C for 4 h. The beads were washed five times with ice-cold PBS and eluted with 1× SDS sample buffer. The eluted proteins were resolved via denaturing SDS/PAGE, transferred to a nylon membrane and blotted with anti-TRPV1 antibody (catalog no. P-19; Santa Cruz Biotechnology) and horseradish perox-

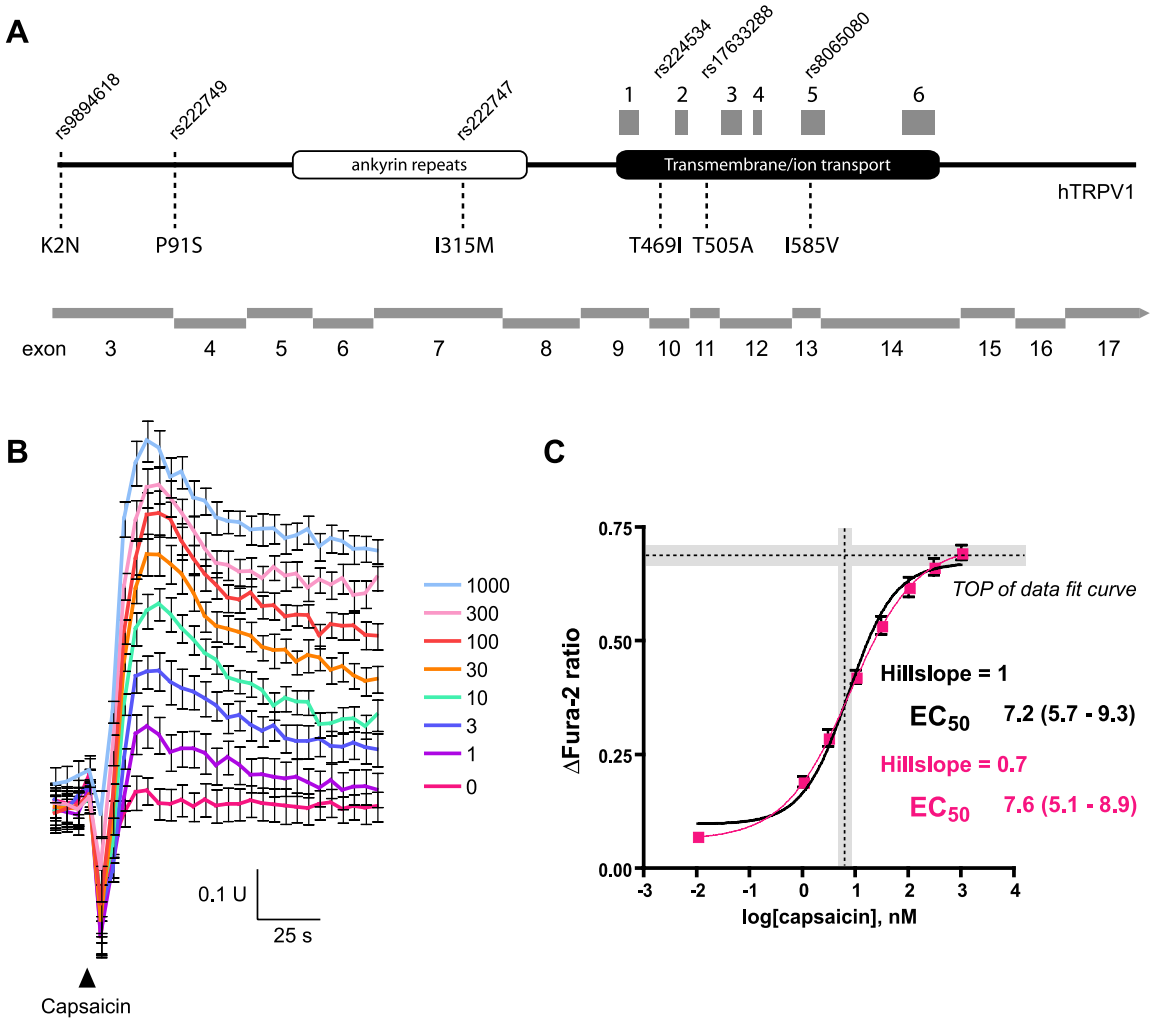

Fig. 1. Nonsynonymous polymorphisms in the human *TRPV1* gene. *A*: diagram of the human TRPV1 protein secondary sequence depicting functional motifs, the location of transmembrane helices 1–6 (gray boxes), and corresponding exons in the human *TRPV1* gene (staggered gray line). The site of the nonsynonymous human single-nucleotide polymorphism (SNP) is represented by the resultant amino acid substitution (dashed lines), and the corresponding SNP designation ("rs" format) is depicted above the cartoon. *B*: representative tracing of the time-dependent increment in fura 2 emission ratio (Em510; in the presence of alternating excitation at 340 and 380 nm) in HEK cells transiently transfected with a human TRPV1 cDNA mutagenized to incorporate a nonsynonymous SNP ($TRPV1^{T505A}$, in this example), in response to various doses of capsaicin from 0 to 1,000 nM. Time of agonist application is denoted by the arrowhead. Error bars reflect SE for 12 wells at each capsaicin dose. A single experiment (i.e., $n = 1$) is depicted. *C*: graphic representation of the 4 parameters comprising the nonlinear regression fit to a sigmoidal dose-response curve (in this example, derived from the data in *B*). When the Hill slope was fixed at unity (i.e., no functional interaction among binding sites), a curve (black tracing) was generated with EC_{50} for capsaicin of 7.2 nM and a *top* of 0.67 (vertical and horizontal dashed lines, respectively, where shaded regions denote 95% confidence intervals). When the variable Hill slope model was applied, and although the calculated EC_{50} value remained nearly unchanged (i.e., 7.6 nM), the curve (pink tracing) was a better fit for the data. See text for further details. EC_{50} (with confidence interval in parentheses) is shown for each regression model. Data for 0 capsaicin were set at 2 logs below the lowest tested dose, in accordance with convention.

idase-conjugated donkey anti-goat IgG secondary antibody. Visualization was via Chemiluminescence Plus reagent (PerkinElmer Life Science).

RNase protection assay. For RNase protection assay, cells were transfected as above (with 6 μg RNA/transfection reaction) and RNA was harvested 48 h later via TRIzol in accordance with the manufacturer's directions (Life Technologies). Solution hybridization was performed with biotinylated antisense riboprobe directed against human TRPV1 (PCR-amplified from full-length human TRPV1 cDNA using the following primer pair: hTRPV1-2261-5′-tcaacaagatcgcacaggag and hTRPV1-2556-3′-gcctgaaactctgcttgacc, where numbers refer to position in NM_080705) and vector backbone [PCR-amplified from plasmid DNA using the following primer pairs: pcDNA3.1-V5HisTOPO-4779-5′ ttgccgggaagctagagtaa and pcDNA3.1-V5HisTOPO-5003-3′ gataacactgcggccaactt; pcDNA3.1-V5HisTOPO-1437-5′ agcgtgaccgctacacttg and pcDNA3.1-V5HisTOPO-1656-3′ aagggcgaaaaaccgtctat, where numbers refer to nucleotide position in pcDNA3.1-V5/HisTOPO as reported by the manufacturer (Invitrogen)]. Detection was achieved via autoradiography.

Image processing and statistical analysis. For quantitation of autoradiograms, exposed films were scanned (Canon LiDE80) and data were reduced using ImageJ (http://rsb.info.nih.gov/ij/; National Institutes of Health) and Excel (Microsoft). For all depicted scans of enhanced chemiluminescence exposures of immunoblots and RNase protection assays, contrast was improved by decreasing the maximum input level from 255 to ~175 (Adobe PhotoShop CS) to mimic the true appearance of the exposed film. For each figure, all depicted lanes are from the same exposure of the same autoradiogram and have been treated identically. All experiments were performed a minimum of three times (see figure legends). Data are expressed as means ± SE (Excel, Microsoft). Statistical significance was ascribed using Student's *t*-test [for correlated samples using raw data, or for independent

samples using normalized data (VassarStats; http://faculty.vassar.edu/lowry/VassarStats.html)]. Where multiple comparisons were performed, the false discovery rate procedure was used (17, 18).

RESULTS

Nonsynonymous polymorphisms in the human TRPV1 gene. We sought nonsynonymous polymorphisms in the human *TRPV1* gene using a public domain SNP database (i.e., dbSNP; www.ncbi.nlm.nih.gov/projects/SNP/) and publication references. We identified five nonsynonymous polymorphisms expected to result in nonconservative amino acid substitution; these are diagrammed in Fig. 1*A*. A sixth site, TRPV1^{I585V}, results in a conservative substitution and was not the subject of initial interest; however, a recent publication addressed potential functional significance of this SNP (32), and it was later included in our analysis. Of note, an additional nonsynonymous SNP designated rs17856604 similarly resulted in a conservative amino acid substitution (TRPV1^{D421E}) and was not investigated; however, it is no longer indexed by this designation. Two of these SNPs affect the intracellular NH_2 terminus of TRPV1: one is in the ankyrin repeat-containing region, and three are in the transmembrane domain. The ankyrin repeat domain is predicted to play a role in mediating protein-protein interactions and perhaps homotetramerization of the channel. TRPV1^{T469I} is expressed on a predicted extracellular loop between membrane-spanning helices one and two, and TRPV1^{I585V} is predicted to reside within membrane-spanning helix five. TRPV1^{T505A} is expressed on an intracellular loop between helices two and three. This general region of TRPV1 confers responsiveness to capsaicin (29). The minor allele frequencies for each of these polymorphisms in the HapMap populations (where data were available) are shown in Table 1.

TRPV1^{WT} and variant forms exhibit similar EC$_{50}$ for capsaicin. HEK293 cells were transiently transfected with a wild-type human TRPV1 cDNA, or one that had undergone site-directed mutagenesis to introduce a polymorphism. In transfected cells loaded with fura 2-AM, capsaicin produced a prompt and dose-dependent increment in intracellular calcium (Fig. 1*B*). Sham treatment (vehicle; 0 nM capsaicin) elicited a negligible effect. [There was no effect of capsaicin in vector-transfected or untransfected cells, and the capsaicin effect was completely dependent on the presence of calcium in the medium (not shown).] The magnitude of the capsaicin response, the increment in fura 2 ratio (Δfura 2 ratio), was quantified for each capsaicin dose as ($r_{max} - r_{initial}$), where $r_{initial}$ represents the mean of the first two data points, and r_{max} was the maximal ratio achieved. A dose-response relationship was plotted for each TRPV1 variant in each experiment, and a sigmoidal dose-response curve was fit (see METHODS) (Fig. 2*C*). Curves were fit with both a fixed Hill slope of 1 and with a variable Hill slope (generally <1), and EC$_{50}$ for capsaicin was computed. In many experiments with TRPV1^{WT} or TRPV1 variants, the data for 1 μM capsaicin deviated substantially from the fit curve; this suggested either a nonspecific effect at this high concentration or the superimposition of an additional mechanism of action. Therefore, curves were fit separately with the data from 1 μM capsaicin either included or excluded. We found no statistically significant differences between the EC$_{50}$ for capsaicin for TRPV1^{WT} and any of the variant forms (Fig. 2). In most cases, the EC$_{50}$ approximated 10 nM. An effect of 1 nM capsaicin was readily detectable in our assay (i.e., Fig. 1*C* and data not shown); however, there was no effect of capsaicin at 0.1 nM ($n = 2$; data not shown). This was lower than was observed by Smart et al. (69) at standard pH (7.4) using a similar platform; this group also reported Hill coefficients in excess of 2 for capsaicin under similar conditions. Data from these authors suggested nonspecific effects of capsaicin at concentrations in excess of 1 μM (69).

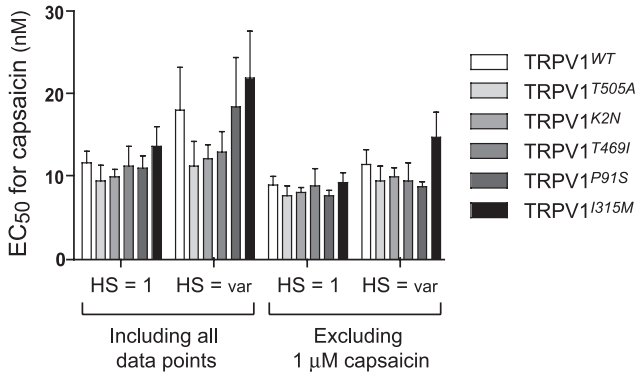

Fig. 2. Calculated EC$_{50}$ for capsaicin in HEK cells transiently transfected with wild-type human TRPV1 (TRPV1^{WT}) or nonsynonymous polymorphic variants of TRPV1. EC$_{50}$ (in nM capsaicin) was calculated using both the fixed [Hill slope (HS) = 1] and variable (HS = var) Hill slope models. Because of a potential concern regarding nonspecific effects at 1,000 nM capsaicin, data including and excluding this dose were reduced in parallel. Values are means ± SE. In terms of EC$_{50}$, none of variants differed significantly from that of wild-type in either model, in the presence or absence of the capsaicin 1 μM data ($n = 8$ for TRPV1^{WT}, 6 for TRPV1^{T505A}, 7 for TRPV1^{K2N}, 5 for TRPV1^{T469I}, 5 for TRPV1^{P91A}, and 5 for TRPV1^{I315M}).

Unlike EC$_{50}$, the curve *top* parameter varied significantly among the expressed TRPV1 polymorphic variants (Fig. 3).

Table 1. *Alleles of the human TRPV1 gene investigated*

SNP ID	Position	Allele	CEU mAF	CHB mAF	JPT mAF	YRI mAF
rs9894618	3442388	TRPV1^{K2N}	?	?	?	?
rs222749	3442123	TRPV1^{P91S}	0.052	0.211	0.284	0
rs222747	3439949	TRPV1^{I315M}	0.183	0.544	0.568	0.058
rs224534	3433451	TRPV1^{T469I}	0.267	0.789	0.864	0.008
rs17633288	3430534	TRPV1^{T505A}	0.017	0	0	0
rs8065080	3427196	TRPV1^{I585V}	0.342	0.589	0.739	0.067

Single-nucleotide polymorphism (SNP) ID is the designation in the National Center for Biotechnology Information (NCBI) SNP data set; position indicates nucleotide position on human chromosome 17 reference assembly as reported by NCBI. Allele denotes the consequence of the polymorphism at the amino acid level in the format TRPV1$^{[major\ allele][residue\ number][minor\ allele]}$. mAF is minor allele frequency in each of the principal HapMap study populations (where available) including CEU (CEPH; Utah residents with ancestry from northern and western Europe), CHB (Han Chinese in Beijing, China), JPT (Japanese in Tokyo, Japan), and YRI (Yoruba in Ibadan, Nigeria).

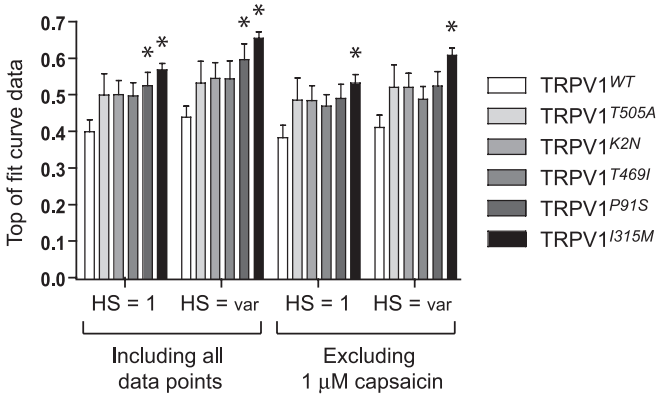

Fig. 3. Calculated *top* parameter of the fit sigmoidal dose-response curve for capsaicin in HEK cells transiently transfected with wild-type human TRPV1 (TRPV1^{WT}) or nonsynonymous polymorphic variants of TRPV1. The *top* parameter of the fit curve for each polymorphic variant was computed using models as in Fig. 2. The *top* parameter for the TRPV1^{I315M} variant exceeded that of TRPV1^{WT} in all models, whereas that of TRPV1^{P19S} exceeded wild-type only when all data points were included. The false discovery rate procedure was applied for multiple comparisons (see METHODS). *Statistical significance with respect to TRPV1^{WT}.

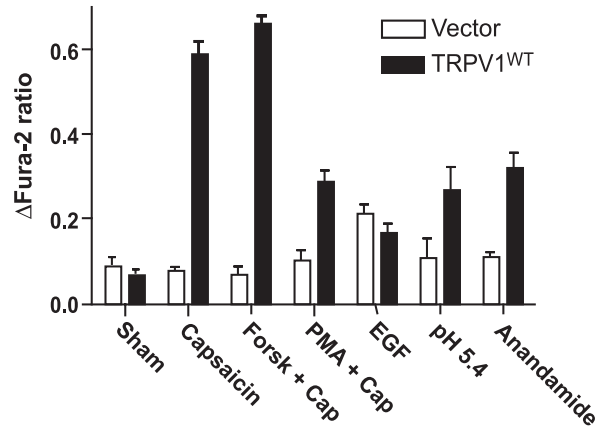

Fig. 4. Effect of TRPV1 agonists on calcium signaling in vector- or TRPV1^{WT}-transfected HEK cells. HEK cells were transfected with TRPV1^{WT} or with empty vector and treated with the indicated agonists (100 nM capsaicin, 100 nM EGF, pH 5.4, or 10 μM anandamide) for ~120 s. For pretreatment experiments (i.e., Forsk+Cap and PMA+Cap), cells received PMA (100 nM) or forskolin (10 nM) for 30 min before medium supplementation with capsaicin. Maximal increment in fura 2 ratio is depicted (n = 3 for each condition). Forskolin or PMA alone exerted no effect (data not shown). Forskolin significantly potentiated the effect of capsaicin, whereas PMA abrogated it.

Irrespective of constraint of the Hill slope to unity, or inclusion of the capsaicin 1 μM data, the TRPV1^{I315M} variant exhibited a more robust maximal effect of capsaicin. Similar findings were noted for the TRPV1^{P91S} variant, but only when all data points were included.

Cells transfected with TRPV1^{P91S} and TRPV1^{I315M} exhibit enhanced responsiveness to anandamide. We sought a second TRPV1 agonist to confirm this relationship. We tested vector- and TRPV1-transfected HEK293 cells with a panel of known TRPV1 agonists. EGF was used as an activator of phospholipase Cγ to alleviate the tonic phosphoinositol-4,5-bisphosphate-dependent inhibition of TRPV1 channel function (55). The activator of protein kinase A, forskolin, was predicted to potentiate the capsaicin response (8, 20, 44, 57), as was the activator of protein kinase C, PMA (3, 41, 54). In our model, forskolin modestly potentiated the effect of capsaicin (Fig. 4). Unexpectedly, pretreatment with the activator of protein kinase C, PMA, inhibited the capsaicin response. This may be a consequence of our longer PMA pretreatment interval (i.e., 10 min), or the use of confluent monolayers; an analogous context-dependent bidirectional regulatory effect on TRPV1 has recently been shown for phosphatidylinositol (4,5)-bisphosphate (39), reconciling prior conflicting observations (55, 72). EGF, low pH (5.4), and anandamide, the endogenous cannabinoid, all modestly activated calcium transients in TRPV1-transfected cells. Of note, the effect of EGF was also observed in the vector-transfected control cells and was therefore independent of TRPV1; the pH and anandamide effects, in contrast, required TRPV1 expression. The effect of anandamide on TRPV1^{P91S} and TRPV1^{I315M} was then compared with TRPV1^{WT}. The anandamide effect was more robust in the TRPV1^{P91S} and TRPV1^{I315M} variants than in TRPV1^{WT} (Fig. 5). Vehicle treatment alone produced no response in vector or TRPV1- or variant TRPV1-transfected cells.

TRPV1^{P91S} and TRPV1^{I315M} proteins are expressed at higher levels following transfection. Based on the more robust response of TRPV1^{I315M} and perhaps TRPV1^{P91S} to capsaicin in the absence of an effect on EC_{50} for the agonist, and based on the differing response to anandamide, we hypothesized that channel abundance might account for the differences among variants. We quantified total expression of each variant following transient transfection and also determined the relative expression at the plasma membrane using cell-surface biotinylation. Relative to TRPV1^{WT}, the variants TRPV1^{I315M} and TRPV1^{P91S} were expressed at higher levels in total lysates (by 82 ± 25 and 89 ± 18%, respectively) and in avidin-affinity precipitates derived from biotinylated transfectants (by 110 ± 40 and 140 ± 40%, respectively) (Fig. 6).

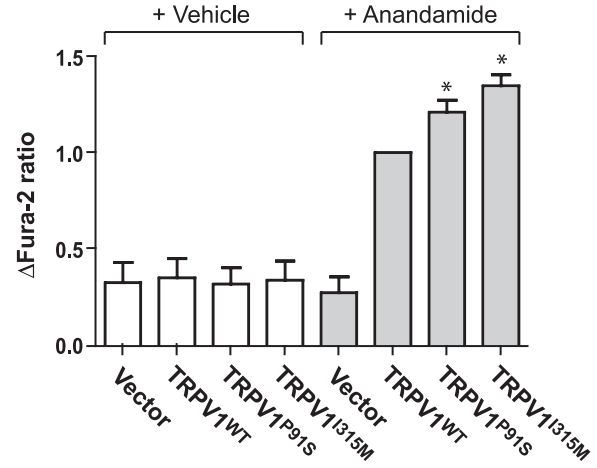

Fig. 5. Effect of anandamide treatment on TRPV1^{WT} and selected TRPV1 SNPs exhibiting increased capsaicin responsiveness. HEK cells were transfected with empty vector control, TRPV1^{WT}, or with either of the SNP-containing variants exhibiting increased responsiveness to capsaicin in Fig. 3 (TRPV1^{P91S} or TRPV1^{I315M}) and then treated with anandamide (10 μM) for ~120 s. To minimize interexperimental variability in the magnitude of the anandamide response (n = 3), data were normalized to the anandamide effect on TRPV1^{WT}. The effect of this agonist on both TRPV1^{P91S} and TRPV1^{I315M} exceeded that of wild-type in each of the 3 experiments and in the aggregated data shown. *Statistical significance with respect to TRPV1^{WT} in the presence of anandamide treatment.

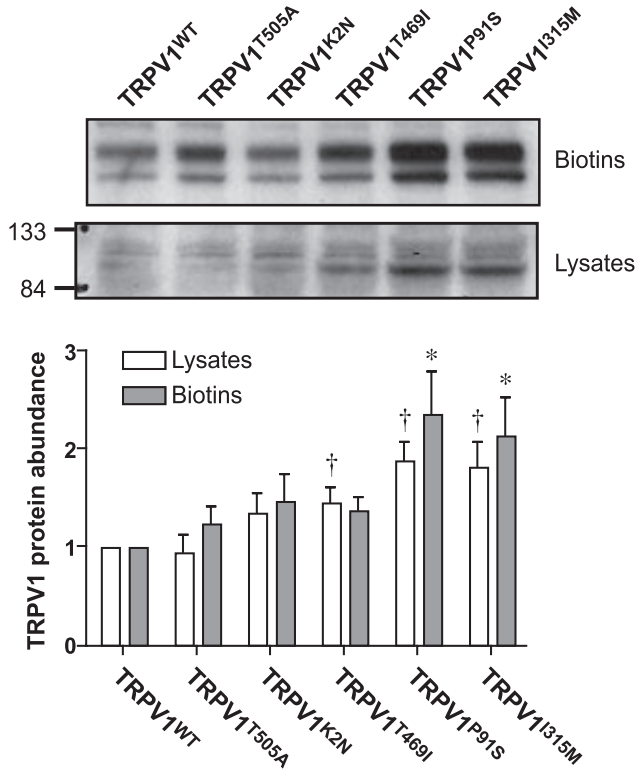

Fig. 6. Expression at the protein level for TRPV1^{WT} and SNP-containing variants. Expression of TRPV1 or variant TRPV1 was determined by anti-TRPV1 immunoblotting of either cell surface-expressed proteins [in avidin-affinity precipitates prepared from surface-biotinylated TRPV1 transient transfectants *top* blot] or of whole-cell lysates (*bottom* blot). Data from 4–5 experiments, depending on experimental condition, are quantified (*bottom*) and normalized to TRPV1^{WT}. For statistical analysis, data are expressed as raw densitometry values (to avoid excluding the variability in TRPV1^{WT}). Student's *t*-test was performed with correlated samples and the false discovery procedure for multiple comparisons. *,†: Statistical significance with respect to TRPV1^{WT} in biotinylated avidin-affinity precipitates and in whole-cell lysates, respectively.

TRPV1^{I315M} exhibits greater expression at the mRNA level following transfection. Because nonsynonymous SNPs can influence mRNA transcription and stability in vivo, we sought to determine whether a component of the increased expression of TRPV1^{I315M} variant could be accounted for by increased expression at the mRNA level. HEK293 cells were transiently transfected with TRPV1^{WT} or variant forms as in our other studies. RNA was harvested and subjected to RNase protection assay with a labeled antisense riboprobe directed against human TRPV1. Expression of the TRPV1^{I315M} and TRPV1^{K2N} variants exceeded that of control by a modest degree (i.e., by 17 and 8%, respectively) (Fig. 7).

TRPV1 haplotype structure can inform investigations into functional consequences of SNPs. With an increasing understanding of the haplotype structure of the human genome comes an appreciation of the interdependent nature of SNPs. SNPs are likely to be coinherited along with adjacent SNPs that reside within the same haplotype block; that is, these often lengthy stretches of genomic sequence are only infrequently subject to recombination. Therefore, we sought to determine which TRPV1 polymorphisms were likely to operate in concert on expression of TRPV1. Figure 8 depicts the haplotype blocks for each of the four diverse human populations represented in the HapMap data set, projected on to the genomic structure of human *TRPV1*. In the Caucasian study population (CEU), the TRPV1^{I315M} and TRPV1^{T469I} polymorphisms may cosegregate; they map to the same haplotype block. In this population, the minor allele frequencies for TRPV1^{I315M} and TRPV1^{T469I} are similar at 0.18 and 0.27, respectively (see Table 1). Also, the linkage disequilibrium between these two SNPs in this population is high ($D' = 0.87$, where D' is an index of genetic linkage, spanning 0 to 1, that is normalized to allele frequency). For the haplotype block including these SNPs, five relatively abundant haplotypes constitute 97.5% of the all possible genomic variation at this locus (data not shown). The TRPV1^{I315M} and TRPV1^{T469I} SNPs coexist in only one of these five possible blocks, which accounted for 15.8% of sequenced alleles from the CEU (Caucasian) HapMap population. Therefore, we tested the effect on TRPV1 function of a combination of these two polymorphisms. We found that the EC_{50} of the TRPV1^{I315M} and TRPV1^{T469I} variants, and of TRPV1^{WT}, did not differ from that of TRPV1$^{I315M/T469I}$, the double-mutant ($n = 3$; data not shown). In addition, although we again found that the *top* of the fit curve for TRPV1^{I315M} exceeded that of TRPV1^{WT} ($n = 3$; $P \simeq 0.01$; data not shown), the effect of the double-mutant TRPV1$^{I315M/T469I}$ was intermediate and not statistically different from either ($n = 3$; data not shown).

In similar fashion, although not residing on the same haplotype block, the TRPV1^{T469I} SNP exhibits relatively strong linkage disequilibrium with a sixth nonsynonymous polymor-

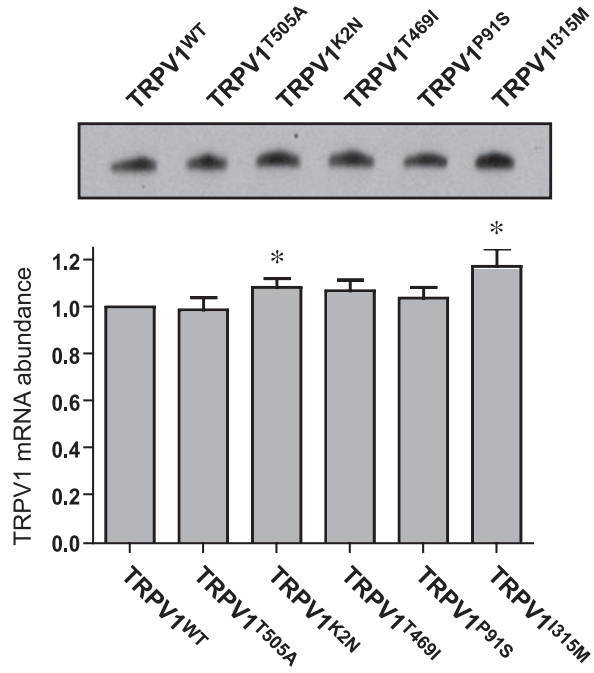

Fig. 7. Expression at the mRNA level for TRPV1^{WT} and SNP-containing variants. Expression of TRPV1 or variant TRPV1 was determined by RNase protection assay. The protected fragment for a representative experiment is depicted (blot) above quantified data from 4 independent experiments. When data were expressed as raw densitometry values and Student's *t*-test was performed with correlated samples, none of the polymorphic variants differed from TRPV1^{WT}. When data were normalized within each experiment to TRPV1^{WT}, abundance of TRPV1^{K2N} and TRPV1^{I315M} exceeded that of TRPV1^{WT} by a statistically significant but a very modest degree (8 ± 4 and 17 ± 8%, respectively). *Statistical significance with respect to TRPV1^{WT}.

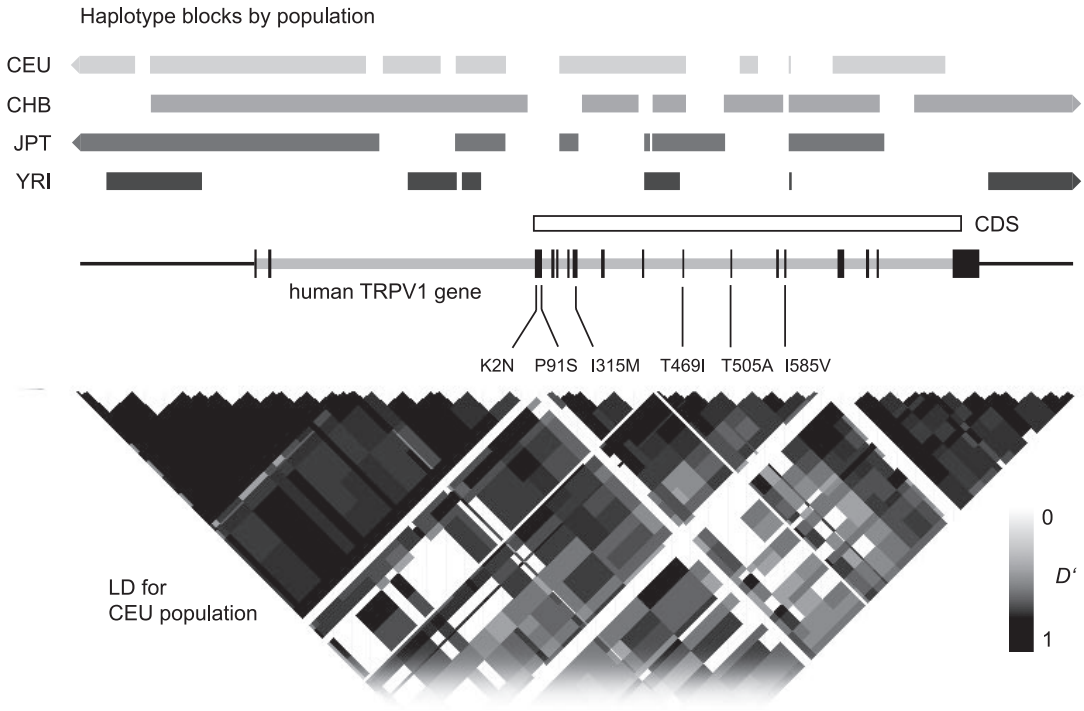

Fig. 8. Relation of nonsynonymous SNPs and haplotype blocks within the human *TRPV1* gene. The region in the figure spans nucleotides 3,410,000–3,470,000 of human chromosome 17; the human *TRPV1* gene (so designated, gray line) is punctuated by 17 exons (vertical black bars), a subset of which gives rise to the *TRPV1* coding sequence (CDS; open bar). Exons to which the TRPV1 nonsynonymous variants map are depicted. Haplotype blocks deduced from the HapMap data sets for Utah residents with ancestry from Northern and Western Europe (CEU), Han Chinese in Beijing (CHB), Japanese in Tokyo (JPT), and Yoruba in Ibadan, Nigeria (YRI) are shown above the gene map; some blocks extend beyond the chromosomal region depicted (blocks ending in same-colored arrowheads). It can be inferred that in the CEU (Caucasian) population, $TRPV1^{I315M}$ and $TRPV1^{T469I}$ reside within the same haplotype block and are likely to be coinherited (see text). A plot of linkage disequilibrium (LD; expressed here as D') over this interval was generated using the HapMap data set for the CEU population. High linkage disequilibrium is evident throughout the potential regulatory regions "upstream" of the *TRPV1* gene and over smaller intervals consistent with the haplotype block structure shown above.

phism, $TRPV1^{I585V}$, among the Han Chinese population in the HapMap data set. Owing to the very conservative nature of this latter polymorphism (i.e., isoleucine to valine), we initially did not select it for detailed investigation; however, when haplotype analysis indicated that it was potentially coinherited with the $TRPV1^{T469I}$ SNP in a Chinese population (linkage disequilibrium, D', was 0.77), we tested the combined effect of these two SNPs on TRPV1 function. (Interestingly, the "intervening" nonsynonymous SNP on the diagram, corresponding to $TRPV1^{T505A}$, exhibited a minor allele frequency of 0 in all non-CEU HapMap study populations; therefore, this SNP was not studied in combination with either $TRPV1^{T469I}$ or $TRPV1^{I585V}$). Of note, although there is generally a high degree of concordance between the Japanese and Han Chinese allele frequency in the HapMap data set, there was only very limited linkage disequilibrium ($D' = 0.21$) between the $TRPV1^{T469I}$ and $TRPV1^{I585V}$ SNPs in the Japanese population. With respect to the $TRPV1^{I585V}$ SNP, the disparity in minor allele frequency among the diverse HapMap study populations is so great that the minor allele in the Caucasian (CEU) population (i.e., Val^{585}) actually represents the major allele in the Han Chinese study population (see Table 1). However, $TRPV1^{T469I}$, $TRPV1^{I585V}$, and $TRPV1^{T469I/I585V}$ did not differ from $TRPV1^{WT}$ in terms of either EC_{50} for capsaicin or other fit parameters of the capsaicin sigmoidal dose-response curve ($n = 3$; data not shown).

TRPV1 polymorphisms potentially conferring type 1 diabetes in a murine model markedly impact TRPV1 function. A pair of nonsynonymous SNPs in the murine *TRPV1* gene (giving rise to murine $TRPV1^{P322A/D734E}$) was recently described in the NOD mouse model of type 1 diabetes, where *TRPV1* may represent the diabetes risk gene in this naturally arising mutant (58). Because these polymorphisms affect amino acids that are conserved across all mammalian and avian species investigated, we tested their effect in the context of the human TRPV1 cDNA. Interestingly, when four-parameter sigmoidal dose-response curves were generated for $hTRPV1^{P322A/D734E}$ and $hTRPV1^{WT}$, the EC_{50} for capsaicin was not significantly affected (14.3 ± 2.1 vs. 10.9 ± 0.4; $P = 0.09$); the *top* and *bottom* of the fit curves were also not impacted (Fig. 9*A*). However, the Hill slope (or Hill coefficient), the steepness of the dose-response curve, was dramatically impacted by the double mutation and was nearly twice that of the wild-type (1.3 ± 0.1 vs. 0.7 ± 0.4; $P = 0.005$) (Fig. 9*B*). Thus a NOD-like human TRPV1 variant was hyporesponsive to capsaicin at low doses (below the EC_{50}) and hyperresponsive at higher doses (Fig. 9*B*). To put this anomaly into perspective, the Hill slope for the capsaicin dose-response was unaffected by incorporation of any of the human polymorphisms we had investigated (Fig. 9*C*), and in none of these individual assays ($n = 42$ separate experiments) did the Hill slope exceed unity (individual data not shown).

DISCUSSION

We sought SNPs that would impact function of TRPV1 in vitro and, potentially, in vivo. Monogenic human diseases associated with point mutations have generally resulted in functional disruption or aberrant trafficking of the gene product, and we initially considered nonsynonymous SNPs as an extension of this paradigm. Clinically significant human polymorphisms, however, need not be defined so narrowly. Accruing evidence suggests that genetic polymorphisms may exert major effects simply by influencing the level of expression of the gene product, independent of its function. To this end, polymorphisms may alter transcription, mRNA stability, or protein half-life. Copy-number polymorphisms, where the number of alleles varies among individuals, affect at least 12% of the genome (59) and account for nearly one-fifth of all detected genetic variations (74); in such cases, the disease state is mediated through altered expression of a normal protein (e.g., Ref. 4). Individual variation in gene expression has long been recognized, and the expression level of individual gene products is hereditary (15, 46, 65, 71, 84). Therefore, it is reasonable to conclude that much of intersubject phenotypic variation will be encoded by polymorphisms that influence levels of gene expression. We postulate that TRPV^{I315M} and perhaps TRPV1^{P91S} are examples of this type. These two polymorphisms resulted in markedly increased abundance of the variant TRPV1 protein at the level of whole-cell expression, and at the level of expression at the cell surface, in our heterologous expression model. Although there was also a very modest increment in TRPV1^{I315M} mRNA level in this model (~17%), it is doubtful that it is sufficient to account for the marked change in protein expression (>100%). Definitive demonstration will require independent testing of allele-specific expression in human subjects. Thus far, there are no data examining the level of TRPV1 expression in any human tissue as a function of allele although this would be of interest. *TRPV1* was not among the genes exhibiting differential expression in lymphoblastoid cells derived from subjects of various ethnicities (71); however, it is unclear whether TRPV1 is expressed in this tissue.

Because SNPs are not inherited in isolation, haplotype structure can be used to further inform investigations into the functional consequences of polymorphic variants. Using utilities and data in the public domain (www.hapmap.org), we show that the TRPV1^{I315M} and TRPV1^{T469I} alleles reside on the same ~7-kb haplotype block in Utah residents with ancestry from Northern and Western Europe (i.e., HapMap CEU population). In genomic DNA, they are separated by ~6.5 kb, exhibit strong linkage disequilibrium, and are likely coinherited in this population. Although the allelic frequencies of both of these SNP variants are much higher in Asian populations [e.g., Japanese in Tokyo, Japan (HapMap JPT population) and Han Chinese in Beijing, China (HapMap CHB population)], they are not predicted to reside on the same haplotype blocks in these populations and are therefore much less likely to be

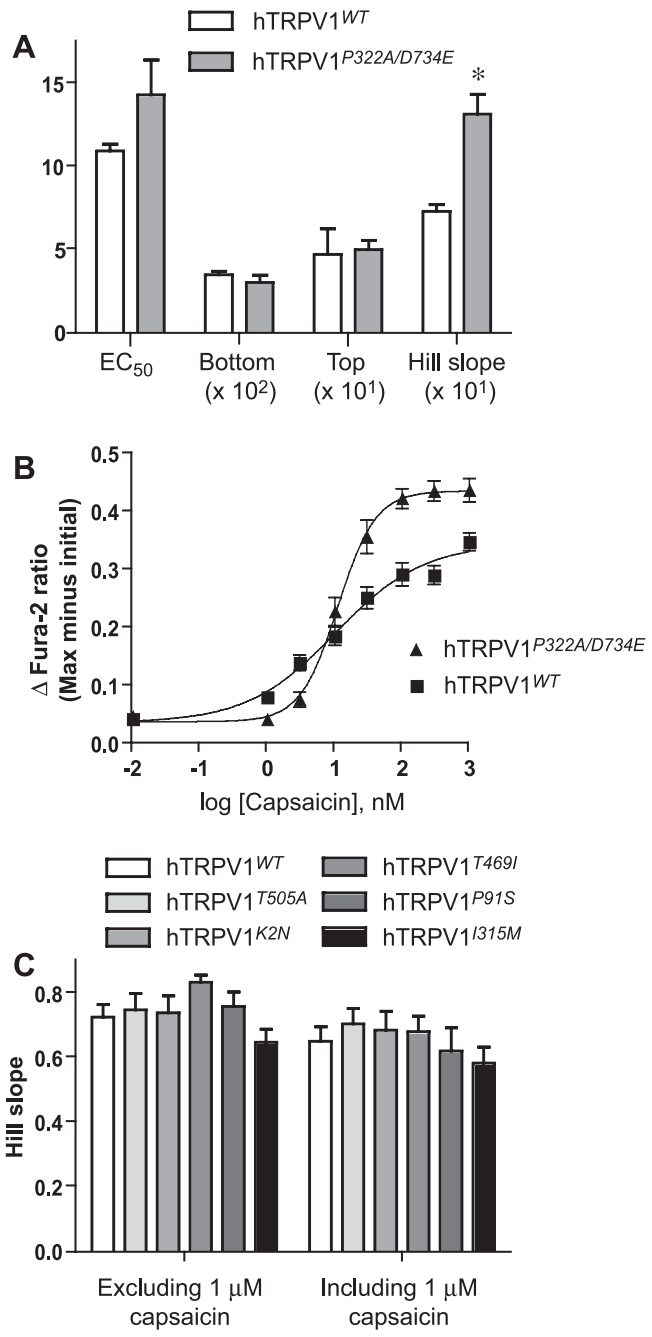

Fig. 9. Effect on TRPV1 function of 2 linked nonsynonymous polymorphisms potentially causal for a type 1 diabetes-like syndrome in the nonobese diabetic (NOD) mouse model. A recent report identified a mutation/polymorphism in each of 2 highly conserved amino acid residues in the murine *TRPV1* gene in the NOD mouse model (58); neurons derived from dorsal root ganglia of mice of this strain were hyporesponsive to capsaicin. The 2 polymorphisms were engineered into the human TRPV1 cDNA, generating TRPV1$^{P322A/D734E}$. *A*: results of 4-parameter curve fit for a nonlinear regression (with unconstrained Hill slope) of the capsaicin dose-response for HEK cells transfected with either TRPV1^{WT} or the polymorphic variant, TRPV1$^{P322A/D734E}$ ($n = 3$ separate experiments). EC_{50} likely did not differ (14 ± 2 vs. 11 ± 0.4; $P = 0.09$); however, the Hill slope for the variant was dramatically elevated relative to wild-type (1.3 ± 0.1 vs. 0.7 ± 0.4; $P = 0.005$). Note that some parameters were scaled by a factor of 10 (*top*, Hill slope) or 100 (*bottom*) to share the same *y*-axis. *Statistical significance with respect to TRPV1^{WT}. *B*: representative capsaicin dose-response curves for HEK cells transfected with TRPV1^{WT} or with the polymorphic variant, TRPV1$^{P322A/D734E}$, showing the "steeper" nature of the dose-response relationship in the TRPV1$^{P322A/D734E}$-transfected cells. *C*: calculated Hill slope values for all capsaicin dose-response experiments (excluding those depicted in *A*) with TRPV1^{WT} and with the human SNP-containing variants for comparison; unlike TRPV1$^{P332A/D734E}$, all are $<<1$, and no significant differences were seen.

coinherited. When both SNPs were introduced into human TRPV1, giving rise to the TRPV1$^{T469I/I315M}$ variant, response of the channel to capsaicin was indistinguishable from TRPV1^{WT} or from either single mutant (data not shown).

A second SNP combination was also tested. In an earlier analysis using HapMap-supplied data (c. 2006), the rs224534 (TRPV1^{T469I}) and rs8065080 (TRPV1^{I585V}) polymorphisms were predicted to reside on the same haplotype block in the Japanese HapMap population (data not shown); however, more recent and comprehensive analysis did not support this view (i.e., Fig. 8). Nonetheless, there was a high degree of linkage disequilibrium between the TRPV1^{T469I} and TRPV1^{I585V} SNPs in the Japanese population ($D' = 0.77$), so these were tested in combination. (Of note, the intervening nonsynonymous SNP, giving rise to TRPV1^{T505A}, is extremely uncommon and was not tested in combination.) In terms of capsaicin responsiveness, we found no novel properties attributable to the combination of both polymorphisms. Interestingly, the major alleles of these polymorphisms, TRPV1^{T469I} and TRPV1^{I585V}, in the HapMap Caucasian population (CEU) are actually the minor alleles in the Chinese and Japanese populations. That is, the tested TRPV1$^{T469I/I585V}$ variant is predicted to represent the most common genotype in both Asian populations.

Two mutations or polymorphisms in the murine *TRPV1* gene were linked to the development of the diabetic phenotype in the NOD mouse model of type 1 diabetes (58). There is remarkable conservation between the human and rodent TRPV1 at the amino acid level (i.e., 87% identity, mouse NP_001001445 vs. human NP_542436, with most sequence divergence residing at the extreme NH_2 and COOH termini of the 839-residue proteins), and the two affected residues are conserved across all mammalian species investigated (58). Razavi et al. (58) tested intact NOD mice and their tissues for capsaicin sensitivity. The NOD mice were less responsive than control mice to foot pad injection of an irritating dose of capsaicin, based on observed biting and licking of the affected extremity (58). Neurons of the dorsal root ganglia isolated from NOD mice were also less responsive to capsaicin than were corresponding neurons isolated from the control mice; however, these neurons retained an intact response to KCl, suggesting specificity of the capsaicin effect (58). We tested the effect of a human variant corresponding to the NOD mutant by generating hTRPV1$^{P322A/D734E}$. Although three of four parameters defining the sigmoidal dose-response relationship for capsaicin were unaffected (including EC_{50} for capsaicin), there was a striking alteration in the "steepness" of this dose-response; the Hill slope for the "diabetic" variant was nearly twice that of wild-type TRPV1 (Fig. 9*B*) or any of the other tested polymorphic variants (Fig. 9*C*). This relationship conferred diminished capsaicin sensitivity at low doses (i.e., 1 and 3 nM capsaicin) and an augmented capsaicin response above the EC_{50}. In contrast, Razavi et al. (58) described reduced capsaicin responsiveness of the NOD dorsal root ganglion neurons across the full dose range tested (i.e., 500 nM-100 μM capsaicin). This discrepancy may reflect differences in cell type (dorsal root ganglion neurons vs. HEK cells), model system (native vs. heterologous expression), assay design (single-cell vs. monolayer), or clone background (human vs. murine). Of note, neither of the mutated residues is predicted to impact capsaicin binding or response based on its location (21, 29–31, 38, 83). Thus far, polymorphisms in these residues have not been described in human populations; however, they might have substantial implications for the phenotype of pain sensitivity or neurogenic inflammation.

The relationship between TRPV1 and diabetes warrants comment. Razavi and colleagues (58) further showed that *TRPV1*$^{-/-}$ mice exhibit increased insulin sensitivity relative to *TRPV1*$^{+/+}$ mice and that genetic reconstitution of wild-type TRPV1 in the NOD mouse model restored insulin sensitivity. Gram et al. (23) made a complementary observation in a second diabetic model; this group observed that pharmacological destruction of capsaicin-sensitive (TRPV1-positive) sensory afferent nerve fibers blocked development of the type 2 diabetic-like state in the Zucker diabetic fatty rat. Whereas TRPV1 may impact diabetes, other studies suggest the converse: that the diabetic state may alter the morphology and/or physiology of TRPV1-containing sensory afferents (e.g., Refs. 19, 25, 52, 56).

A role for TRPV1 in the predisposition to human diabetes has not yet been demonstrated. In five recent large-scale genome-wide association studies, no polymorphisms in the human *TRPV1* gene, or in adjacent genes on human chromosome 17, were linked to type 2 diabetes (Refs. 64, 66, 68, 73, 87 and online supporting materials); the presence of a modest effect or a subset-specific effect cannot be excluded, however, nor can a role for TRPV1 in type 1 diabetes.

Little has been written about physiological effects of polymorphisms in the human *TRPV1* gene. Kim and colleagues (32) observed that a number of variables influence sensitivity to experimentally-induced pain. American female subjects of European descent with the TRPV1^{I585V} allele exhibited shorter cold withdrawal times (i.e., increased sensitivity to cold-induced pain) than did those with the wild-type allele (32). For these studies, subjects were instructed to submerse their hands in ice water up to the wrists with repeated clenching and unclenching until the pain reached an "unbearable level" (maximum 180 s). There were no allele-specific differences in the subjects' ability to tolerate elevated temperatures in similarly designed studies. We initially did not investigate this polymorphism in detail because of the highly conservative nature of the amino acid substitution and because data from Hayes and colleagues (24) previously suggested that the channel encoded by the TRPV1^{I585V} allele exhibited a normal functional response to agonists in vitro. We did, however, incorporate it into our investigation of the linked SNP, TRPV1^{T469I}.

Both the TRPV1^{I315M} and TRV1^{T469I} alleles are overrepresented in South Asian populations (i.e., Han Chinese and Japanese subjects from Tokyo in the HapMap cohort), and TRPV1^{I315M} is associated with increased expression of the channel at both the mRNA and protein levels in the present study. TRPV1 likely plays a major role in integrating nociceptive signals, particularly in the contexts of inflammatory and neuropathic pain (reviewed in Refs. 13 and 78). A body of literature underscores racial differences in the perception and/or response to painful stimuli (reviewed in Ref. 50); for example, two clinical studies found that Asian patients may require less postoperative analgesia than European patients (26, 75). This phenomenon may be attributed to purely psychological or cultural factors and has not been replicated in all studies (86); nonetheless, it raises the intriguing possibility that genetic polymorphisms, such as those investigated here, may

account for or contribute to a racial difference in pain threshold or tolerance.

GRANTS

This work was supported by the American Heart Association, the Department of Veterans Affairs, and the National Institute of Diabetes and Digestive and Kidney Diseases.

REFERENCES

1. **Acs G, Palkovits M, Blumberg PM.** Comparison of [^{3}H]resiniferatoxin binding by the vanilloid (capsaicin) receptor in dorsal root ganglia, spinal cord, dorsal vagal complex, sciatic and vagal nerve and urinary bladder of the rat. *Life Sci* 55: 1017–1026, 1994.
2. **Acs G, Palkovits M, Blumberg PM.** Specific binding of [^{3}H]resiniferatoxin by human and rat preoptic area, locus ceruleus, medial hypothalamus, reticular formation and ventral thalamus membrane preparations. *Life Sci* 59: 1899–1908, 1996.
3. **Ahern GP.** Activation of TRPV1 by the satiety factor oleoylethanolamide. *J Biol Chem* 278: 30429–30434, 2003.
4. **Aitman TJ, Dong R, Vyse TJ, Norsworthy PJ, Johnson MD, Smith J, Mangion J, Roberton-Lowe C, Marshall AJ, Petretto E, Hodges MD, Bhangal G, Patel SG, Sheehan-Rooney K, Duda M, Cook PR, Evans DJ, Domin J, Flint J, Boyle JJ, Pusey CD, Cook HT.** Copy number polymorphism in Fcgr3 predisposes to glomerulonephritis in rats and humans. *Nature* 439: 851–855, 2006.
5. **Akiba Y, Nakamura M, Nagata H, Kaunitz JD, Ishii H.** Acid-sensing pathways in rat gastrointestinal mucosa. *J Gastroenterol* 37: 133–138, 2002.
6. **Barrett JC, Fry B, Maller J, Daly MJ.** Haploview: analysis and visualization of LD and haplotype maps. *Bioinformatics* 21: 263–265, 2005.
7. **Bevan S, Hothi S, Hughes G, James IF, Rang HP, Shah K, Walpole CS, Yeats JC.** Capsazepine: a competitive antagonist of the sensory neurone excitant capsaicin. *Br J Pharmacol* 107: 544–552, 1992.
8. **Bhave G, Zhu W, Wang H, Brasier DJ, Oxford GS, Gereau RW.** cAMP-dependent protein kinase regulates desensitization of the capsaicin receptor (VR1) by direct phosphorylation. *Neuron* 35: 721–731, 2002.
9. **Birder LA, Kanai AJ, de Groat WC, Kiss S, Nealen ML, Burke NE, Dineley KE, Watkins S, Reynolds IJ, Caterina MJ.** Vanilloid receptor expression suggests a sensory role for urinary bladder epithelial cells. *Proc Natl Acad Sci USA* 98: 13396–13401, 2001.
10. **Birder LA, Nakamura Y, Kiss S, Nealen ML, Barrick S, Kanai AJ, Wang E, Ruiz G, De Groat WC, Apodaca G, Watkins S, Caterina MJ.** Altered urinary bladder function in mice lacking the vanilloid receptor TRPV1. *Nat Neurosci* 5: 856–860, 2002.
11. **Bortolotti M, Coccia G, Grossi G, Miglioli M.** The treatment of functional dyspepsia with red pepper. *Aliment Pharmacol Ther* 16: 1075–1082, 2002.
12. **Calignano A, Katona I, Desarnaud F, Giuffrida A, La Rana G, Mackie K, Freund TF, Piomelli D.** Bidirectional control of airway responsiveness by endogenous cannabinoids. *Nature* 408: 96–101, 2000.
13. **Caterina MJ, Julius D.** The vanilloid receptor: a molecular gateway to the pain pathway. *Annu Rev Neurosci* 24: 487–517, 2001.
14. **Caterina MJ, Schumacher MA, Tominaga M, Rosen TA, Levine JD, Julius D.** The capsaicin receptor: a heat-activated ion channel in the pain pathway. *Nature* 389: 816–824, 1997.
15. **Cheung VG, Conlin LK, Weber TM, Arcaro M, Jen KY, Morley M, Spielman RS.** Natural variation in human gene expression assessed in lymphoblastoid cells. *Nat Genet* 33: 422–425, 2003.
16. **Cortright DN, Crandall M, Sanchez JF, Zou T, Krause JE, White G.** The tissue distribution and functional characterization of human VR1. *Biochem Biophys Res Commun* 281: 1183–1189, 2001.
17. **Curran-Everett D.** Multiple comparisons: philosophies and illustrations. *Am J Physiol Regul Integr Comp Physiol* 279: R1–R8, 2000.
18. **Curran-Everett D, Benos D.** Guidelines for reporting statistics in journals published by the American Physiological Society. *Am J Physiol Cell Physiol* 287: C243–C245, 2004.
19. **Davidson EP, Coppey LJ, Yorek MA.** Activity and expression of the vanilloid receptor 1 (TRPV1) is altered by long-term diabetes in epineurial arterioles of the rat sciatic nerve. *Diabetes Metab Res Rev* 22: 211–219, 2006.
20. **De Petrocellis L, Harrison S, Bisogno T, Tognetto M, Brandi I, Smith GD, Creminon C, Davis JB, Geppetti P, Di Marzo V.** The vanilloid receptor (VR1)-mediated effects of anandamide are potently enhanced by the cAMP-dependent protein kinase. *J Neurochem* 77: 1660–1663, 2001.
21. **Gavva NR, Klionsky L, Qu Y, Shi L, Tamir R, Edenson S, Zhang TJ, Viswanadhan VN, Toth A, Pearce LV, Vanderah TW, Porreca F, Blumberg PM, Lile J, Sun Y, Wild K, Louis JC, Treanor JJ.** Molecular determinants of vanilloid sensitivity in TRPV1. *J Biol Chem* 279: 20283–20295, 2004.
22. **Goso C, Evangelista S, Tramontana M, Manzini S, Blumberg PM, Szallasi A.** Topical capsaicin administration protects against trinitrobenzene sulfonic acid-induced colitis in the rat. *Eur J Pharmacol* 249: 185–190, 1993.
23. **Gram DX, Ahren B, Nagy I, Olsen UB, Brand CL, Sundler F, Tabanera R, Svendsen O, Carr RD, Santha P, Wierup N, Hansen AJ.** Capsaicin-sensitive sensory fibers in the islets of Langerhans contribute to defective insulin secretion in Zucker diabetic rat, an animal model for some aspects of human type 2 diabetes. *Eur J Neurosci* 25: 213–223, 2007.
24. **Hayes P, Meadows HJ, Gunthorpe MJ, Harries MH, Duckworth DM, Cairns W, Harrison DC, Clarke CE, Ellington K, Prinjha RK, Barton AJ, Medhurst AD, Smith GD, Topp S, Murdock P, Sanger GJ, Terrett J, Jenkins O, Benham CD, Randall AD, Gloger IS, Davis JB.** Cloning and functional expression of a human orthologue of rat vanilloid receptor-1. *Pain* 88: 205–215, 2000.
25. **Hong S, Wiley JW.** Early painful diabetic neuropathy is associated with differential changes in the expression and function of vanilloid receptor 1. *J Biol Chem* 280: 618–627, 2005.
26. **Houghton IT, Aun CS, Gin T, Lau JT.** Inter-ethnic differences in postoperative pethidine requirements. *Anaesth Intensive Care* 20: 52–55, 1992.
27. **Hwang SW, Cho H, Kwak J, Lee SY, Kang CJ, Jung J, Cho S, Min KH, Suh YG, Kim D, Oh U.** Direct activation of capsaicin receptors by products of lipoxygenases: endogenous capsaicin-like substances. *Proc Natl Acad Sci USA* 97: 6155–6160, 2000.
28. **Hwang SW, Oh U.** Hot channels in airways: pharmacology of the vanilloid receptor. *Curr Opin Pharmacol* 2: 235–242, 2002.
29. **Jordt SE, Julius D.** Molecular basis for species-specific sensitivity to "hot" chili peppers. *Cell* 108: 421–430, 2002.
30. **Jung J, Hwang SW, Kwak J, Lee SY, Kang CJ, Kim WB, Kim D, Oh U.** Capsaicin binds to the intracellular domain of the capsaicin-activated ion channel. *J Neurosci* 19: 529–538, 1999.
31. **Jung J, Lee SY, Hwang SW, Cho H, Shin J, Kang YS, Kim S, Oh U.** Agonist recognition sites in the cytosolic tails of vanilloid receptor 1. *J Biol Chem* 277: 44448–44454, 2002.
32. **Kim H, Neubert JK, San Miguel A, Xu K, Krishnaraju RK, Iadarola MJ, Goldman D, Dionne RA.** Genetic influence on variability in human acute experimental pain sensitivity associated with gender, ethnicity and psychological temperament. *Pain* 109: 488–496, 2004.
33. **Kuzhikandathil EV, Wang H, Szabo T, Morozova N, Blumberg PM, Oxford GS.** Functional analysis of capsaicin receptor (vanilloid receptor subtype 1) multimerization and agonist responsiveness using a dominant negative mutation. *J Neurosci* 21: 8697–8706, 2001.
34. **Liedtke W, Choe Y, Marti-Renom MA, Bell AM, Denis CS, Sali A, Hudspeth AJ, Friedman JM, Heller S.** Vanilloid receptor-related osmotically activated channel (VR-OAC), a candidate vertebrate osmoreceptor. *Cell* 103: 525–535, 2000.
35. **Liedtke W, Friedman JM.** Abnormal osmotic regulation in trpv4−/− mice. *Proc Natl Acad Sci USA* 100: 13698–13703, 2003.
36. **Liu L, Lo Y, Chen I, Simon SA.** The responses of rat trigeminal ganglion neurons to capsaicin and two nonpungent vanilloid receptor agonists, olvanil and glyceryl nonamide. *J Neurosci* 17: 4101–4111, 1997.
37. **Liu L, Simon SA.** A rapid capsaicin-activated current in rat trigeminal ganglion neurons. *Proc Natl Acad Sci USA* 91: 738–741, 1994.
38. **Lu G, Henderson D, Liu L, Reinhart PH, Simon SA.** TRPV1b: a functional human vanilloid receptor splice variant. *Mol Pharmacol* 67: 1119–1127, 2005.
39. **Lukacs V, Thyagarajan B, Varnai P, Balla A, Balla T, Rohacs T.** Dual regulation of TRPV1 by phosphoinositides. *J Neurosci* 27: 7070–7080, 2007.
40. **Lundberg JM, Saria A.** Capsaicin-induced desensitization of airway mucosa to cigarette smoke, mechanical and chemical irritants. *Nature* 302: 251–253, 1983.
41. **Mandadi S, Numazaki M, Tominaga M, Bhat MB, Armati PJ, Roufogalis BD.** Activation of protein kinase C reverses capsaicin-induced

calcium-dependent desensitization of TRPV1 ion channels. *Cell Calcium* 35: 471–478, 2004.
42. **McNamara FN, Randall A, Gunthorpe MJ.** Effects of piperine, the pungent component of black pepper, at the human vanilloid receptor (TRPV1). *Br J Pharmacol* 144: 781–790, 2005.
43. **Mezey E, Toth ZE, Cortright DN, Arzubi MK, Krause JE, Elde R, Guo A, Blumberg PM, Szallasi A.** Distribution of mRNA for vanilloid receptor subtype 1 (VR1), and VR1-like immunoreactivity, in the central nervous system of the rat and human. *Proc Natl Acad Sci USA* 97: 3655–3660, 2000.
44. **Mohapatra DP, Nau C.** Desensitization of capsaicin-activated currents in the vanilloid receptor TRPV1 is decreased by the cyclic AMP-dependent protein kinase pathway. *J Biol Chem* 278: 50080–50090, 2003.
45. **Montell C.** The TRP superfamily of cation channels. *Sci STKE* 2005: re3, 2005.
46. **Morley M, Molony CM, Weber TM, Devlin JL, Ewens KG, Spielman RS, Cheung VG.** Genetic analysis of genome-wide variation in human gene expression. *Nature* 430: 743–747, 2004.
47. **Motulsky H, Christopoulos A.** *Fitting Models to Biological Data Using Linear and Nonlinear Regression: A Practical Guide to Curve Fitting*. San Diego, CA: GraphPad Software, Inc, 2005.
48. **Myrdal SE, Steyger PS.** TRPV1 regulators mediate gentamicin penetration of cultured kidney cells. *Hear Res* 204: 170–182, 2005.
49. **Nilius B, Voets T, Peters J.** TRP channels in disease. *Sci STKE* 2005: re8, 2005.
50. **Njobvu P, Hunt I, Pope D, Macfarlane G.** Pain amongst ethnic minority groups of South Asian origin in the United Kingdom: a review. *Rheumatology (Oxford)* 38: 1184–1187, 1999.
51. **Oh U, Hwang SW, Kim D.** Capsaicin activates a nonselective cation channel in cultured neonatal rat dorsal root ganglion neurons. *J Neurosci* 16: 1659–1667, 1996.
52. **Pare M, Albrecht PJ, Noto CJ, Bodkin NL, Pittenger GL, Schreyer DJ, Tigno XT, Hansen BC, Rice FL.** Differential hypertrophy and atrophy among all types of cutaneous innervation in the glabrous skin of the monkey hand during aging and naturally occurring type 2 diabetes. *J Comp Neurol* 501: 543–567, 2007.
53. **Parlani M, Conte B, Goso C, Szallasi A, Manzini S.** Capsaicin-induced relaxation in the rat isolated external urethral sphincter: characterization of the vanilloid receptor and mediation by CGRP. *Br J Pharmacol* 110: 989–994, 1993.
54. **Premkumar LS, Qi ZH, Van Buren J, Raisinghani M.** Enhancement of potency and efficacy of NADA by PKC-mediated phosphorylation of vanilloid receptor. *J Neurophysiol* 91: 1442–1449, 2004.
55. **Prescott ED, Julius D.** A modular PIP2 binding site as a determinant of capsaicin receptor sensitivity. *Science* 300: 1284–1288, 2003.
56. **Rashid MH, Inoue M, Bakoshi S, Ueda H.** Increased expression of vanilloid receptor 1 on myelinated primary afferent neurons contributes to the antihyperalgesic effect of capsaicin cream in diabetic neuropathic pain in mice. *J Pharmacol Exp Ther* 306: 709–717, 2003.
57. **Rathee PK, Distler C, Obreja O, Neuhuber W, Wang GK, Wang SY, Nau C, Kress M.** PKA/AKAP/VR-1 module: a common link of Gs-mediated signaling to thermal hyperalgesia. *J Neurosci* 22: 4740–4745, 2002.
58. **Razavi R, Chan Y, Afifiyan FN, Liu XJ, Wan X, Yantha J, Tsui H, Tang L, Tsai S, Santamaria P, Driver JP, Serreze D, Salter MW, Dosch HM.** TRPV1+ sensory neurons control beta cell stress and islet inflammation in autoimmune diabetes. *Cell* 127: 1123–1135, 2006.
59. **Redon R, Ishikawa S, Fitch KR, Feuk L, Perry GH, Andrews TD, Fiegler H, Shapero MH, Carson AR, Chen W, Cho EK, Dallaire S, Freeman JL, Gonzalez JR, Gratacos M, Huang J, Kalaitzopoulos D, Komura D, MacDonald JR, Marshall CR, Mei R, Montgomery L, Nishimura K, Okamura K, Shen F, Somerville MJ, Tchinda J, Valsesia A, Woodwark C, Yang F, Zhang J, Zerjal T, Armengol L, Conrad DF, Estivill X, Tyler-Smith C, Carter NP, Aburatani H, Lee C, Jones KW, Scherer SW, Hurles ME.** Global variation in copy number in the human genome. *Nature* 444: 444–454, 2006.
60. **Rinder J, Szallasi A, Lundberg JM.** Capsaicin-, resiniferatoxin-, and lactic acid-evoked vascular effects in the pig nasal mucosa in vivo with reference to characterization of the vanilloid receptor. *Pharmacol Toxicol* 78: 327–335, 1996.
61. **Rosenbaum T, Simon SA.** TRPV1 receptors and signal transduction. In: *TRP Ion Channel Function in Sensory Transduction and Cellular Signaling Cascades*, edited by Liedtke WB and Heller S. Boca Raton, FL: CRC, 2007.
62. **Sanchez JF, Krause JE, Cortright DN.** The distribution and regulation of vanilloid receptor VR1 and VR1 5′ splice variant RNA expression in rat. *Neuroscience* 107: 373–381, 2001.
63. **Sasamura T, Sasaki M, Tohda C, Kuraishi Y.** Existence of capsaicin-sensitive glutamatergic terminals in rat hypothalamus. *Neuroreport* 9: 2045–2048, 1998.
64. **Saxena R, Voight BF, Lyssenko V, Burtt NP, de Bakker PI, Chen H, Roix JJ, Kathiresan S, Hirschhorn JN, Daly MJ, Hughes TE, Groop L, Altshuler D, Almgren P, Florez JC, Meyer J, Ardlie K, Bengtsson K, Isomaa B, Lettre G, Lindblad U, Lyon HN, Melander O, Newton-Cheh C, Nilsson P, Orho-Melander M, Rastam L, Speliotes EK, Taskinen MR, Tuomi T, Guiducci C, Berglund A, Carlson J, Gianniny L, Hackett R, Hall L, Holmkvist J, Laurila E, Sjogren M, Sterner M, Surti A, Svensson M, Tewhey R, Blumenstiel B, Parkin M, Defelice M, Barry R, Brodeur W, Camarata J, Chia N, Fava M, Gibbons J, Handsaker B, Healy C, Nguyen K, Gates C, Sougnez C, Gage D, Nizzari M, Gabriel SB, Chirn GW, Ma Q, Parikh H, Richardson D, Ricke D, Purcell S.** Genome-wide association analysis identifies loci for type 2 diabetes and triglyceride levels. *Science* 316: 1331–1336, 2007.
65. **Schadt EE, Monks SA, Drake TA, Lusis AJ, Che N, Colinayo V, Ruff TG, Milligan SB, Lamb JR, Cavet G, Linsley PS, Mao M, Stoughton RB, Friend SH.** Genetics of gene expression surveyed in maize, mouse and man. *Nature* 422: 297–302, 2003.
66. **Scott LJ, Mohlke KL, Bonnycastle LL, Willer CJ, Li Y, Duren WL, Erdos MR, Stringham HM, Chines PS, Jackson AU, Prokunina-Olsson L, Ding CJ, Swift AJ, Narisu N, Hu T, Pruim R, Xiao R, Li XY, Conneely KN, Riebow NL, Sprau AG, Tong M, White PP, Hetrick KN, Barnhart MW, Bark CW, Goldstein JL, Watkins L, Xiang F, Saramies J, Buchanan TA, Watanabe RM, Valle TT, Kinnunen L, Abecasis GR, Pugh EW, Doheny KF, Bergman RN, Tuomilehto J, Collins FS, Boehnke M.** A genome-wide association study of type 2 diabetes in Finns detects multiple susceptibility variants. *Science* 316: 1341–1345, 2007.
67. **Sharif Naeini R, Witty MF, Seguela P, Bourque CW.** An N-terminal variant of Trpv1 channel is required for osmosensory transduction. *Nat Neurosci* 9: 93–98, 2006.
68. **Sladek R, Rocheleau G, Rung J, Dina C, Shen L, Serre D, Boutin P, Vincent D, Belisle A, Hadjadj S, Balkau B, Heude B, Charpentier G, Hudson TJ, Montpetit A, Pshezhetsky AV, Prentki M, Posner BI, Balding DJ, Meyre D, Polychronakos C, Froguel P.** A genome-wide association study identifies novel risk loci for type 2 diabetes. *Nature* 445: 881–885, 2007.
69. **Smart D, Jerman JC, Gunthorpe MJ, Brough SJ, Ranson J, Cairns W, Hayes PD, Randall AD, Davis JB.** Characterisation using FLIPR of human vanilloid VR1 receptor pharmacology. *Eur J Pharmacol* 417: 51–58, 2001.
70. **Smith GD, Gunthorpe MJ, Kelsell RE, Hayes PD, Reilly P, Facer P, Wright JE, Jerman JC, Walhin JP, Ooi L, Egerton J, Charles KJ, Smart D, Randall AD, Anand P, Davis JB.** TRPV3 is a temperature-sensitive vanilloid receptor-like protein. *Nature* 418: 186–190, 2002.
71. **Spielman RS, Bastone LA, Burdick JT, Morley M, Ewens WJ, Cheung VG.** Common genetic variants account for differences in gene expression among ethnic groups. *Nat Genet* 39: 226–231, 2007.
72. **Stein AT, Ufret-Vincenty CA, Hua L, Santana LF, Gordon SE.** Phosphoinositide 3-kinase binds to TRPV1 and mediates NGF-stimulated TRPV1 trafficking to the plasma membrane. *J Gen Physiol* 128: 509–522, 2006.
73. **Steinthorsdottir V, Thorleifsson G, Reynisdottir I, Benediktsson R, Jonsdottir T, Walters GB, Styrkarsdottir U, Gretarsdottir S, Emilsson V, Ghosh S, Baker A, Snorradottir S, Bjarnason H, Ng MC, Hansen T, Bagger Y, Wilensky RL, Reilly MP, Adeyemo A, Chen Y, Zhou J, Gudnason V, Chen G, Huang H, Lashley K, Doumatey A, So WY, Ma RC, Andersen G, Borch-Johnsen K, Jorgensen T, van Vliet-Ostaptchouk JV, Hofker MH, Wijmenga C, Christiansen C, Rader DJ, Rotimi C, Gurney M, Chan JC, Pedersen O, Sigurdsson G, Gulcher JR, Thorsteinsdottir U, Kong A, Stefansson K.** A variant in CDKAL1 influences insulin response and risk of type 2 diabetes. *Nat Genet* 39: 770–775, 2007.
74. **Stranger BE, Forrest MS, Dunning M, Ingle CE, Beazley C, Thorne N, Redon R, Bird CP, de Grassi A, Lee C, Tyler-Smith C, Carter N, Scherer SW, Tavare S, Deloukas P, Hurles ME, Dermitzakis ET.** Relative impact of nucleotide and copy number variation on gene expression phenotypes. *Science* 315: 848–853, 2007.

75. **Streltzer J, Wade TC.** The influence of cultural group on the undertreatment of postoperative pain. *Psychosom Med* 43: 397–403, 1981.
76. **Strotmann R, Harteneck C, Nunnenmacher K, Schultz G, Plant TD.** OTRPC4, a nonselective cation channel that confers sensitivity to extracellular osmolarity. *Nat Cell Biol* 2: 695–702, 2000.
77. **Szallasi A, Blumberg PM, Annicelli LL, Krause JE, Cortright DN.** The cloned rat vanilloid receptor VR1 mediates both R-type binding and C-type calcium response in dorsal root ganglion neurons. *Mol Pharmacol* 56: 581–587, 1999.
78. **Szallasi A, Cruz F, Geppetti P.** TRPV1: a therapeutic target for novel analgesic drugs? *Trends Mol Med* 12: 545–554, 2006.
79. **Szallasi A, Goso C, Blumberg PM, Manzini S.** Competitive inhibition by capsazepine of [^{3}H]resiniferatoxin binding to central (spinal cord and dorsal root ganglia) and peripheral (urinary bladder and airways) vanilloid (capsaicin) receptors in the rat. *J Pharmacol Exp Ther* 267: 728–733, 1993.
80. **Szallasi A, Nilsson S, Farkas-Szallasi T, Blumberg PM, Hokfelt T, Lundberg JM.** Vanilloid (capsaicin) receptors in the rat: distribution in the brain, regional differences in the spinal cord, axonal transport to the periphery, and depletion by systemic vanilloid treatment. *Brain Res* 703: 175–183, 1995.
81. **Tian W, Fu Y, Wang DH, Cohen DM.** Regulation of TRPV1 by a novel renally expressed rat TRPV1 splice variant. *Am J Physiol Renal Physiol* 290: F117–F126, 2006.
82. **Tominaga M, Tominaga T.** Structure and function of TRPV1. *Pflügers Arch* 451: 143–150, 2005.
83. **Vos MH, Neelands TR, McDonald HA, Choi W, Kroeger PE, Puttfarcken PS, Faltynek CR, Moreland RB, Han P.** TRPV1b overexpression negatively regulates TRPV1 responsiveness to capsaicin, heat and low pH in HEK293 cells. *J Neurochem* 99: 1088–1102, 2006.
84. **Yan H, Yuan W, Velculescu VE, Vogelstein B, Kinzler KW.** Allelic variation in human gene expression (Abstract). *Science* 297: 1143, 2002.
85. **Yiangou Y, Facer P, Dyer NH, Chan CL, Knowles C, Williams NS, Anand P.** Vanilloid receptor 1 immunoreactivity in inflamed human bowel. *Lancet* 357: 1338–1339, 2001.
86. **Zatzick DF, Dimsdale JE.** Cultural variations in response to painful stimuli. *Psychosom Med* 52: 544–557, 1990.
87. **Zeggini E, Weedon MN, Lindgren CM, Frayling TM, Elliott KS, Lango H, Timpson NJ, Perry JR, Rayner NW, Freathy RM, Barrett JC, Shields B, Morris AP, Ellard S, Groves CJ, Harries LW, Marchini JL, Owen KR, Knight B, Cardon LR, Walker M, Hitman GA, Morris AD, Doney AS, McCarthy MI, Hattersley AT.** Replication of genome-wide association signals in UK samples reveals risk loci for type 2 diabetes. *Science* 316: 1336–1341, 2007.
88. **Zhu Y, Wang Y, Wang DH.** Diuresis and natriuresis caused by activation of VR1-positive sensory nerves in renal pelvis of rats. *Hypertension* 46: 992–997, 2005.
89. **Zygmunt PM, Petersson J, Andersson DA, Chuang H, Sorgard M, Di Marzo V, Julius D, Hogestatt ED.** Vanilloid receptors on sensory nerves mediate the vasodilator action of anandamide. *Nature* 400: 452–457, 1999.